The effects of surface roughness on the aerodynamic drag coefficient of vehicles

Kemal Ermiş[1*], Mehmet Çalışkan[1], and Anıl Okan[2]

0000-0002-7835-9414, 0000-0003-3110-2731, 0000-0002-7977-1937

[1] *Department of Mechanical Engineering, Sakarya University of Applied Sciences, Sakarya, 54187, Turkey*
[2] *Graduate Education Institute, Automotive Engineering, Sakarya University, Sakarya, 54187, Turkey*

Abstract

In this study, the effects of surface roughness differences of vehicle coating materials (paint, paste, special applications, etc.) on the aerodynamic drag coefficient were investigated using the finite element method. For this, aerodynamic drag forces and aerodynamic drag coefficients for speeds between 40-150 km/hours were calculated for a 1/20 scale vehicle designed by a package program by defining the body parts and front-rear window parts separately and assigning pre-calculated roughness values suitable in the industry, and the results were presented through graphs and visuals. Using three different paint roughness values (low, medium, and high), and one commonly used Teflon (fluoropolymer) coating, it was observed that the aerodynamic resistance coefficient increased with increasing roughness levels. Relative to the aerodynamic resistance coefficient for the lowest paint roughness value, the aerodynamic resistance coefficient for the medium roughness value showed an increase of 0.000612529%, the aerodynamic resistance coefficient for the high roughness value showed an increase of 0.00104783%, and the aerodynamic resistance coefficient for the fluoropolymer coating showed an increase of 0.091195826%. In addition, the distribution of the pressure forces on the vehicle hood and windscreen were also observed in the study. It was observed that the pressure forces, which were approaching maximum on the front bumper, windscreen and side mirrors, were reduced over the rear windscreen area due to separated flow. It was also observed that the aerodynamic resistance force can be reduced by processes such as angular improvements to be made in the front bumper and vehicle windscreens.

Keywords: Aerodynamics; Drag coefficient; Surface roughness; CFD; Automotive

1. Introduction

The aerodynamic drag coefficient (Cd), which is one of the most prominent topics regarding resistances affecting vehicle movements, has been the subject of a significant amount of past and current research. Studies on reducing the aerodynamic drag coefficient have an important place among the studies carried out in the automotive sector today. Today two main approaches used to determine the aerodynamic drag coefficient of a vehicle are wind tunnel testing and computational fluid dynamics analysis. Although wind tunnel tests give reliable results, they are time-consuming and expensive. A number of methods have been used to determine the aerodynamic drag coefficient. The most common method used to determine the aerodynamic drag coefficients of vehicles is by means of wind tunnels. However, recently, with the development of technology, CFD (Computational Fluid Dynamics) methods

have been used to determine this coefficient through the use of package programs. These new methods lead to gains both in terms of cost and time. The work in recent years can be summarized as follows. Asım et al. (2019) carried out a study on the effect of the surface roughness of truck trailers on the aerodynamic drag coefficient using the finite element method. They found that the aerodynamic drag coefficient increased at high speeds [1]. Mallick (2014) carried out studies on the effects of surface roughness of cylindrical objects on the aerodynamic drag coefficient [2]. Qi and Lui (2011) examined the effect that making changes to the trailer structure had on the aerodynamic drag coefficient [3]. Rohatgi (2012) showed that changing the form of the rear body of an off-road vehicle can lead to an improved aerodynamic drag coefficient. His results showed an improvement of 26% [4]. Solmaz and Icingur (2011) analyzed a bus model with the CFD method using a package program and found an aerodynamic drag coefficient of

0.65 according to the experimental results and 0.66 according to the CFD analysis results [5]. Rakibul Hassan et al. (2014) studied numerical analysis on aerodynamic drag reduction of racing cars using the Favre-averaged Navier-Stokes equations backed by k–epsilon turbulence model [6]. Aerodynamic optimization must be balanced against such considerations as styling, ergonomics, and soiling [7].

The work in the earliest years can be summarized as follows. Kieffer et al. (2006) carried out experiments on a Mazda brand sports vehicle by means of CFD analysis using the k-epsilon model [8]. They revealed that the front wing design has significant consequences on the ground effect. Aka (2003) carried out experiments on a 1/16 scale passenger vehicle design and prepared a force measurement system. In addition, the dimensionless coefficients and the pressure distribution are calculated on the vehicle. The aerodynamic drag coefficient value was 0.31 that value constitutes a 5% difference compared to the actual value [9]. Beccaria et al. (1999) developed a program called the Hiperroad, which is used in multiprocessor computers. When they tested the Ferrari F5050 vehicle using this program, which is used for aerodynamic control, they found that the measurements were appropriate [10]. Hucho et al. (1993) carried out studies showing that the Navier – Stokes methods based on the Reynolds number would be more effective in determining the aerodynamic drag coefficient [11]. Hiroyuki Ozawa et al. (1998) 96 Honda studied the aerodynamic characteristics of a solar-powered vehicle. The numerical fluid dynamics method MAC (Markerand - Cell) was used based on the pressure conditions on the vehicle surface. As a result, they encountered a dispersed pressure gauge and therefore suggested, in the aerodynamic analysis of the vehicles, that it would be beneficial to apply multi-directional air currents instead of unidirectional currents [12]. Schenkel (1977) mounted a spoiler on a 3/8 scale vehicle model, and calculated its effects on the drag and lift forces using the wind tunnel method. He examined the effects of placing additional elements in front and behind vehicles on the aerodynamic drag coefficient [13]. Specifics of surface/volume mesh generated, boundary conditions imposed and numerical scheme employed are discussed by Ramakrishnan et al. [14]. Gilhaus (1981) calculated that the added wind reflector reduces the aerodynamic drag coefficient by 14% using a 1/5 scale truck model [15].

Although there are many studies regarding the topic of the aerodynamic drag coefficient in the literature, as shown above, there are not enough studies on the effects of surface roughness on the aerodynamic drag coefficient.

2. Theoretical Foundations

The friction coefficient can be calculated theoretically in laminar flow, but experimental methods are used for the solution in a turbulent flow. Since the coefficient of friction varies over a given surface, the concept of the average coefficient of friction is generally used. In the Eq. (1) expressing the average friction coefficient can be given [16].

$$C_f = \frac{1}{L} \int_0^L C_{f,x} \, dx \tag{1}$$

where C_f is the average coefficient of friction, L is the length, $C_{f,x}$ is the local friction coefficient.

In laminar flow, the surface roughness does not affect the friction coefficient, and the friction coefficient depends on the Reynolds number. However, in turbulent flow, surface roughness can cause the friction coefficient to increase two to three-fold. In order to investigate the effect of surface roughness on the friction coefficient, an Eq.(2) was developed that gives results under certain boundary conditions[16].

$$C_f = \left(1.89 - 1.62\log\frac{\epsilon}{L}\right)^{-2.5} \tag{2}$$

where ϵ is relative roughness, L is plate length in the flow direction.

The ϵ/L value is of great importance when it comes to calculating the results in this formula, which gives results under Re $>10^6$ and $\epsilon/L >10^{-4}$ conditions [16]. This value was studied in the computational fluid dynamics (CFD) analysis.

The graph showing the effect of surface roughness on the friction coefficient in laminar flow with varying Reynolds numbers is given below. As can be seen in Figure 1, the friction coefficient increases with increasing roughness value [16]. With the increase in the friction coefficient, which is one of the two components of the aerodynamic drag coefficient, it is expected that the aerodynamic drag coefficient will naturally increase for turbulent flows.
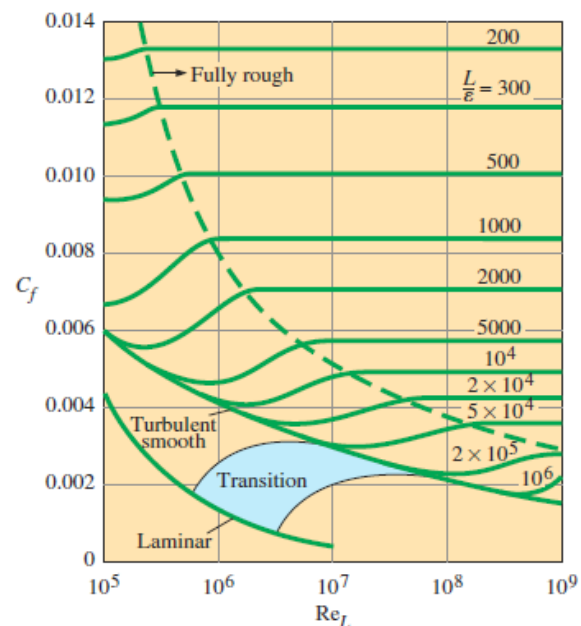

Fig. 1. Effect of surface roughness on friction coefficient in flat plates [17].

3. Materials and Methods

The bodywork of the sample vehicle model used in this study; a

total of five different roughness levels, consisting of three paints with different roughness values, a fluoropolymer coating, and a completely smooth surface, were tested. For the front and rear windows of the vehicle, a constant glass average roughness value of 9.40×10^{-8} m was used [18].

Apart from the values shown in Table.1, the roughness value of the steel material, which is generally preferred in automotive bodywork with the exception of coating materials used in vehicles, varies between 6×10^{-7} m and 8×10^{-7} m [19]. Considering this value, it can be said that a paint material with low roughness has a smaller roughness value than an unpainted vehicle body and will be beneficial in reducing the aerodynamic drag coefficient. The values of the related roughnesses are given in Table1.

Table 1. Used roughness values for measurements.

Scenario	Roughness Height (Ra),m
Paint-1	3.51×10^{-7}
Paint-2	1.03×10^{-6}
Paint-3	1.48×10^{-6}
Fluoropolymer	5.24×10^{-6}
Glass	9.40×10^{-8}

In order to investigate the effects of the vehicular coating materials (paint, putty, etc.) on the aerodynamic drag coefficient, a vehicle model was prepared using the Design Modular program. A virtual wind tunnel was created using the CFD analyses (Ansys Fluent 19.2 program) were made for the five different roughness levels at each speed, with a 10 km/h speed increase in the range of 40 km/h – 150 km/h. The calculated Reynolds Numbers for the velocities and model geometry to be examined are shown in Table 2.

Table 2. Calculated Reynolds Numbers for the velocities and model geometry to be tested.

Flow Length (m)	Speed (m/s)	Speed (km/hour)	Reynolds Number
0.23	11.11	40	1.44×10^5
0.23	13.89	50	1.79×10^5
0.23	16.67	60	2.15×10^5
0.23	19.44	70	2.51×10^5
0.23	22.22	80	2.87×10^5
0.23	25	90	3.23×10^5
0.23	27.78	100	3.59×10^5
0.23	30.56	110	3.95×10^5
0.23	33.33	120	4.31×10^5
0.23	36.11	130	4.67×10^5
0.23	38.89	140	5.02×10^5
0.23	41.67	150	5.38×10^5

Considering the Reynolds number values given in Table 2, the flow around the vehicle can theoretically be considered as turbulent flow at speeds of 140 km/h and 150 km/h, and as transitional flow at other speeds [16].

3.1 Flow Model

The k–epsilon model, which is a two-equation turbulent flow model, stands out with its low cost and practical structure. The disadvantages of the model are that it does not give as accurate results as the k–omega under boundary layer conditions with high roughness and it has low sensitivity in backflows [20]. It was stated that in the Launder and Spalding, k – epsilon model there are two equations; one being k and the other being epsilon, with k representing the kinetic energy of the model [21].

In the k-omega model, k indicates the kinetic energy of the turbulent flow, while omega indicates the energy loss. Since it is a more sensitive model than the k-epsilon model under boundary layer conditions where the flow is more intense, the k-omega turbulent flow model was also used in our analyses. Analyses using the SST k-omega and the reliable k-epsilon solution models yield results with an error of less than 0.5%. In the aerodynamic analysis guide published by SAE (Society of Automotive Engineering), it was shown that the k-omega model gives high accuracy results [22].

3.2 The Finite Element Model and Boundary Conditions

The number of elements and nodes of the model prepared and its specifications are given for this study in Table 3.

Table 3. The model specifications and network data.

| Model type	Viscous (k-omega turbulence model)	
Front surface area (m²)	0.00498449 (1/20 scale)	
Density of air (kg/m³)	1.225	
Temperature (K)	288.16	
Speed(km/hour)	40 – 150	
Viscosity (kg/m*s)	1.7894×10^{-5}	
	Number of Elements	Node Number
Network Data	107365	93935

4. CFD Analysis Results

The aerodynamic drag coefficient (Cd), friction force, convergence graph, and pressure distribution values for the Paint-1 analysis at 11.11 m/s as seen in Figure 2.

The Paint-2 and the Paint-3 analysis are similar to the above figures' processes. Their data have very close results to Paint-1data. The aerodynamic drag coefficient (Cd), friction force, convergence graph, and pressure distribution values for the Fluoropolymer analysis at 11.11 m/s as seen in Figure 3.
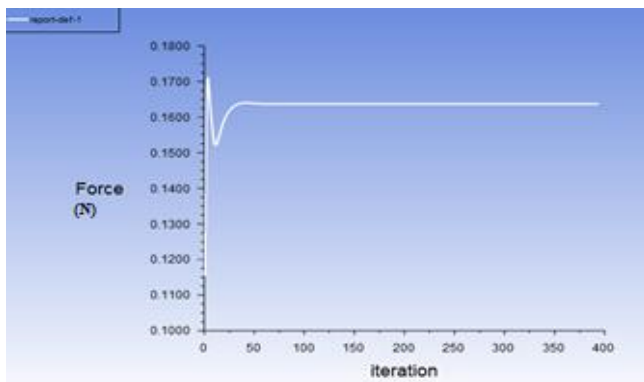
The aerodynamic drag coefficient (Cd) plots show that after 100 iterations, the Cd values remain uniformly constant in both. The friction force graphs show that after about 100 iterations, the friction force values remain the same for both. These give the information that the analyzes were done correctly.
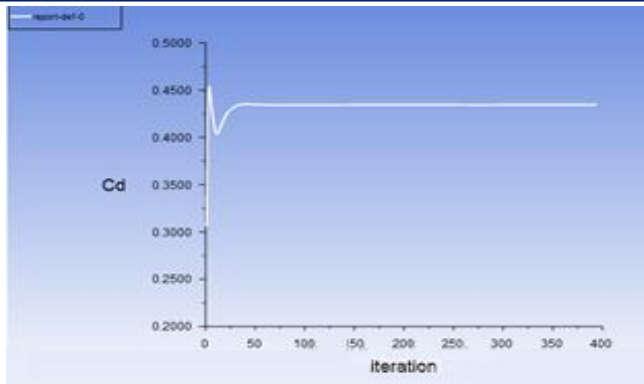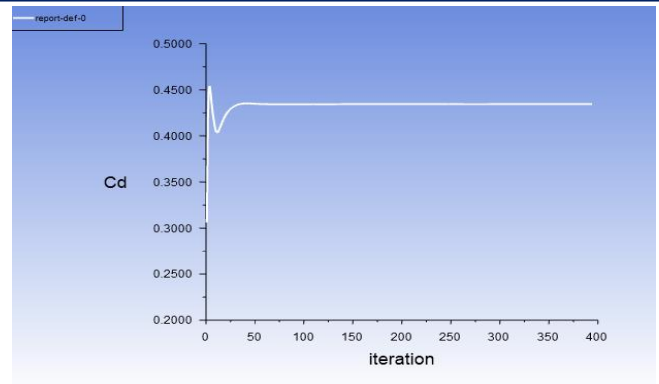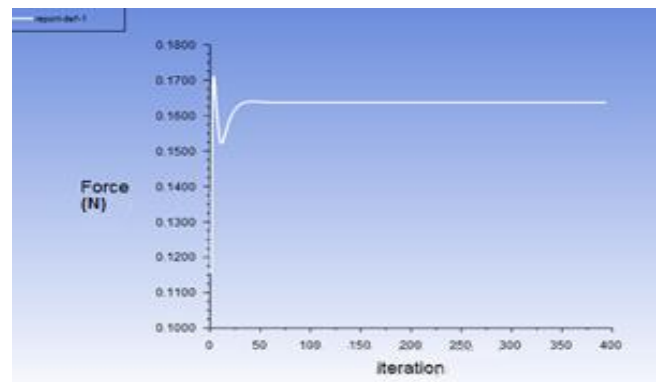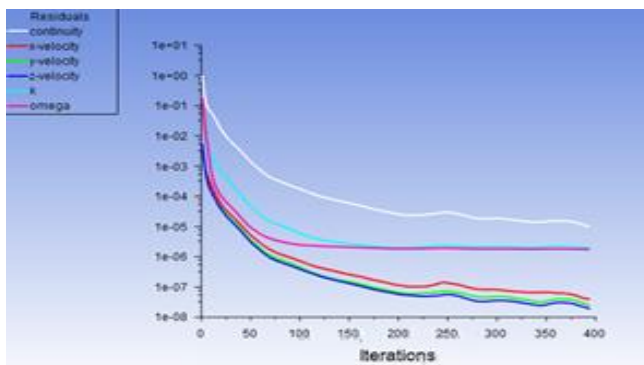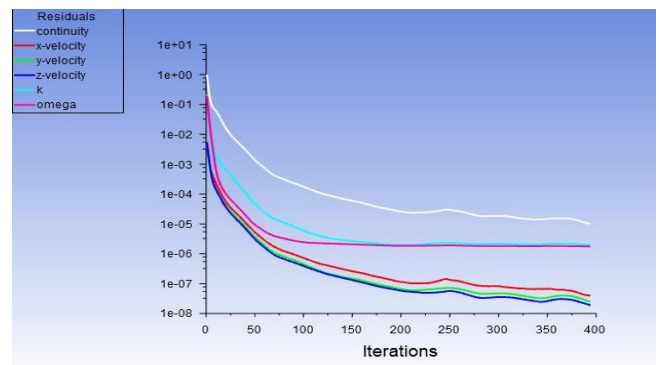
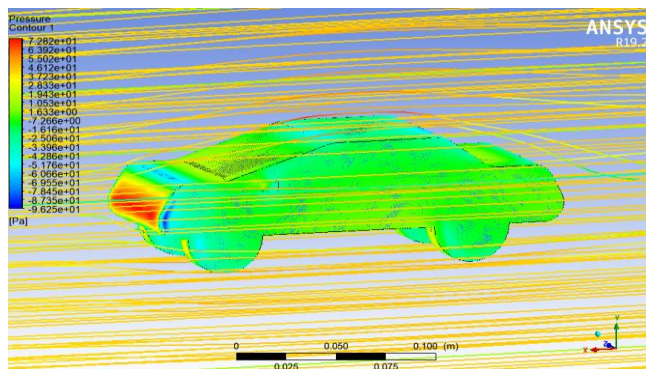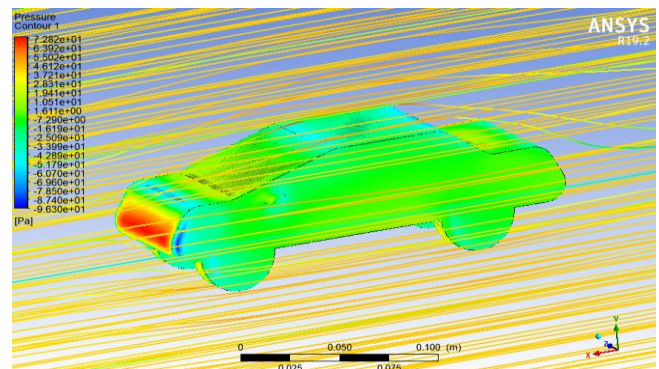Fig. 2. a) The aerodynamic drag coefficient (C_d), b) friction force, c) convergence graph, d) pressure distribution values for the Paint-1 analysis

Fig. 3. a) The aerodynamic drag coefficient (C_d), b) friction force, c) convergence graph, d) pressure distribution values for the Fluoropolymer analysis

Pressure distribution values are given in Figure 2-d and Figure 3-d for Paint-1 coating and fluoropolymer coating, respectively. It is seen that the pressure distribution values of the Paint-1 coating are lower than the Fluoropolymer coating.

As seen in Figure 4, aerodynamic drag forces change in direct proportion to the square of the velocity. While calculating these values, the scale value of 1/20 was taken into account and the front surface area was multiplied by 400 to yield the results seen in the graph. However, due to the very small difference between the values, the change in force relative to the roughness level cannot be fully understood. For this reason, the graph in Figure 6 was used.
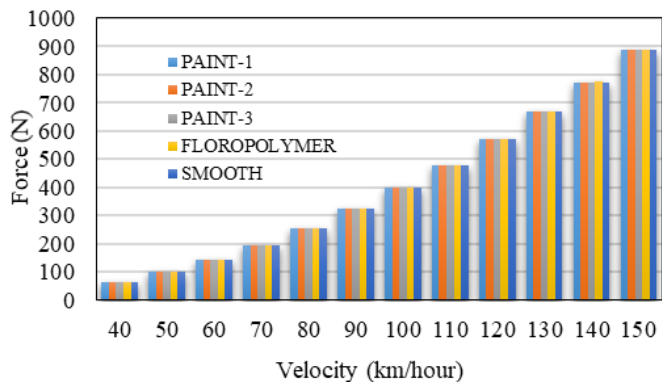

Fig.4. Variation of aerodynamic drag forces at various speeds

The graph in Figure 5 clearly shows the aerodynamic resistance forces at 100 km/h and the change in these forces relative to the hood cover material. As can be seen in Figure 6, both the aerodynamic drag force value and the roughness value were higher for the fluoropolymer coated vehicles.
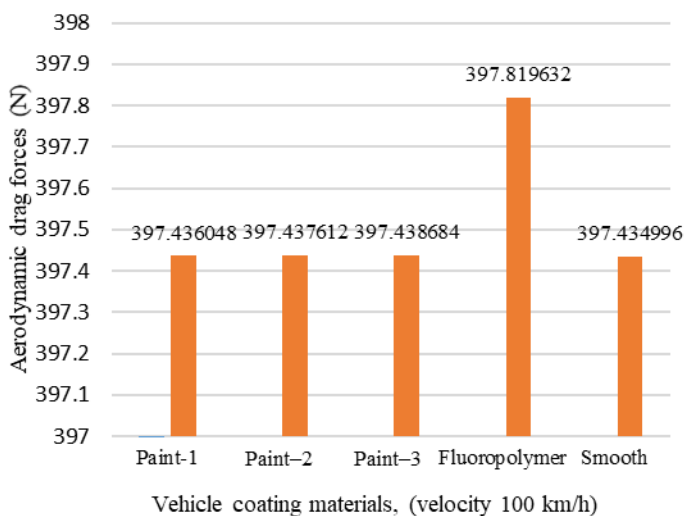

Fig.5. Variation of aerodynamic drag forces at 100 km/h

The aerodynamic drag coefficient value is important for vehicles and forms the basis of the relevant study. Accordingly, the graph showing the changes in the aerodynamic drag coefficient as a result of the forces acting on the vehicle in the range of 40 km/h - 150 km/h, is shown in Figure 6.

As can be seen, the effect of roughness on the aerodynamic drag coefficient becomes more apparent as the speed increases.
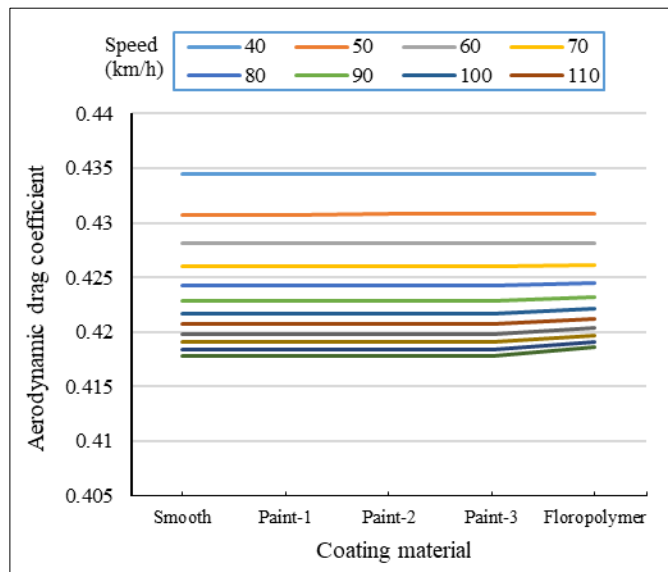

Fig.6. Variation of aerodynamic drag coefficients of coating materials at various speeds

Table 4. Aerodynamic drag force values for different coating and smooth surfaces (no coating)

Speed (km/h)	AERODYNAMIC DRAG FORCE (N)				
	Low Roughness	Mid-Roughess	High Roughness	Fluoro-polymer	Smooth Hood
40	65.480912	65.481280	65.481520	65.483676	65.480664
50	101.492056	101.492648	101.493072	101.500180	101.491680
60	145.271872	145.272584	145.273072	145.297312	145.271388
70	196.596104	196.596900	196.597360	196.661432	196.595468
80	255.825716	255.826776	255.827512	255.960668	255.825244
90	322.778776	322.779592	322.780148	323.015088	322.778528
100	397.436048	397.437612	397.438684	397.819632	397.434996
110	479.794320	479.797640	479.799880	480.378360	479.792320
120	569.525760	569.531000	569.534400	570.340040	569.522880
130	667.271960	667.277440	667.282040	668.364280	667.269200
140	772.725280	772.732480	772.737840	774.151520	772.721080
150	885.875600	885.883520	885.889840	887.690560	885.869800

Aerodynamic drag coefficient (Cd) values calculated by the package program in three different paint roughness values converted to real size according to the vehicle scale as shown in Table 4. As can be seen in Table 4, aerodynamic resistance forces in three different roughness dye values make changes that affect the 2nd or 3rd steps after the comma on average. However, variations in aerodynamic resistance

forces between the smooth body structure and the fluoropolymer coating with high roughness are seen. Accordingly, for a vehicle traveling at a speed of 100 km / h, it is seen that an aerodynamic resistance force difference of 0.97% occurs.

4.1 Mesh independency and structure

As can be seen from Figure 2 a-c and Figure 3a-c graphics, the mesh structure has been converged and as a result, it has been made independent of the mesh. Mesh element quality is controlled at the network structure as shown in Figure 7.

There are 107365 elements and 93935 nodes in the mesh structure. This structure is the hexahedral dominant. In this structure, hexahedral and tetrahedral are used as the main elements. Pyramid and prismatic wedges are used as transition elements.
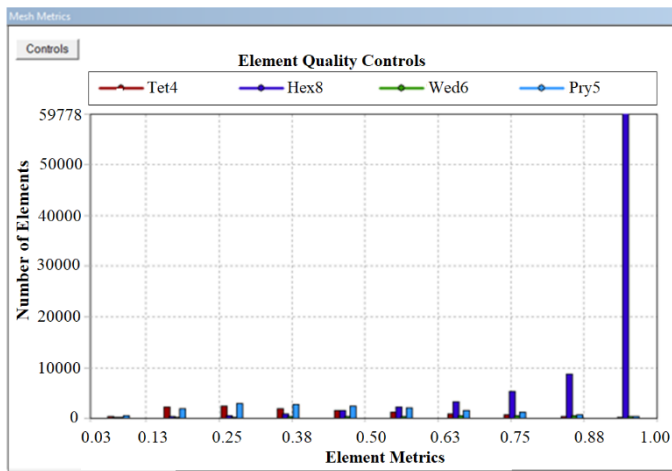

Fig.7. Mesh element quality controls

As seen in Figure 7, 76% of the total elements in the mesh structure are hexahedral, 16% pyramid, 7% tetrahedral, and 1% prismatic wedges.

5. Conclusions and Discussion

A 1/20 scale sample vehicle model was designed using the Design Modular program and by creating the appropriate network structure in the CFD analysis (Ansys 19.2 package) program. Five different body roughness levels and the roughness values of these levels were examined in terms of aerodynamics using the k-omega turbulent flow model within a speed range of 40 km/h – 150 km/h. These roughness values, which are different by 1/1000000 of the meter (m), affected the aerodynamic drag force and aerodynamic drag coefficient values as can be predicted. In these analyzes performed on the aerodynamic drag force and the aerodynamic drag coefficient occurring in the second or third step after the comma as a result of calculations made over the; It creates an average of 0.205% difference between the maximum roughness fluoropolymer coating and the smooth coating with zero roughness.

Although there are differences between the high roughness paint and low roughness paint coating in the fourth or fifth stages after the comma in terms of aerodynamic resistance coefficients, the difference

in the zero roughness value with the fluoropolymer coating starts to occur in the third step comma. Accordingly, according to the low paint roughness value, 0.000612529% increase in aerodynamic resistance coefficient compared to medium roughness value, 0.00104783% increase in aerodynamic resistance coefficient compared to high roughness value and 0.091195826% increase in aerodynamic resistance coefficient according to fluoropolymer roughness value.

According to the data, the coating materials used in vehicles do not cause serious material damage in conditions where the values of 1/1000000 small (micron) of a meter generally used in today's conditions are not exceeded much. However, these differences will increase when considering buses or trucks. They have a large surface area other than automobiles and make more average roads per year.

It was observed that the pressure forces, which were approaching maximum on the front bumper, windscreen, and side mirrors, were reduced over the rear windscreen area due to separated flow. It was also observed that the aerodynamic resistance force can be reduced by processes such as angular improvements to be made in the front bumper and vehicle windscreens. The aerodynamic resistance forces and aerodynamic resistance coefficients that increase with the effect of this pressure can be reduced by the angular inclinations to be given to the front bumper is which leads to a reduction of the forcing acting on it.

Nomenclature

ϵ	: Relative roughness, (m)
CFD	: Computational Fluid Dynamics
C_d	: Aerodynamic drag coefficient (-)
C_f	: Average coefficient of friction (-)
$C_{f,x}\ L$	: Local friction coefficient (-)
	: Length, (m)

Conflict of Interest Statement

The authors declared that there is no conflict of interest in the study.

CRediT Author Statement

Kemal Ermiş: Conceptualization, Supervision, Writing-review & editing,
Mehmet Çalışkan: Methodology, Visualization,
Anıl Okan: Data curation, Formal analysis, Writing-original draft

References

[1] Asim T, Ubbi K, Mishra R, et al. Effect of surface roughness on the aerodynamic performance of an articulated truck-trailer assembly. In: *The 24th Congrès Français de Mécanique (CFM 2019)*. Brest, France, https://rgu-repository.worktribe.com/output/248528 (2019).

[2] Mallick K, Wandera L, Bhattarai N, et al. A Critical Evaluation on the Role of Aerodynamic and Canopy–Surface Conductance Parameterization in SEB and SVAT Models for Simulating Evapotranspiration: A Case Study in the Upper Biebrza National Park Wetland in Poland. *Water 2018, Vol 10, Page 1753* 2018; 10: 1753.

[3] Qi X, Liu Y, Du G, et al. Experimental and Numerical Studies of

Aerodynamic Performance of Trucks. *JHyDy* 2011; 23: 752–758.

[4] Rohatgi US. Methods of Reducing Vehicle Aerodynamic Drag Non-proliferation and National Security/Safeguards and Verification Implementation/Building 197D.

[5] Yakup Içingür. Determination of drag coefficients of various automobile models in a low speed wind tunnel. *Fak Der J Fac Eng Arch Gazi Univ Cilt* 2011; 26: 455–460.

[6] Rakibul Hassan SM, Islam T, Ali M, et al. Numerical Study on Aerodynamic Drag Reduction of Racing Cars. *Procedia Engineering* 2014; 90: 308–313.

[7] Frank T, Turney J. Aerodynamics of Commercial Vehicles. *Lecture Notes in Applied and Computational Mechanics* 2016; 79: 195–210.

[8] Kieffer W, Moujaes S, Armbya N. CFD study of section characteristics of Formula Mazda race car wings. *Mathematical and Computer Modelling* 2006; 43: 1275–1287.

[9] Aka H. Study On Aerodynamic Characteristics of a Passenger Car in A Wind Tunnel (M.Sc. Thesis) . Gazi University, 2003.

[10] Beccaria M, Buresti G, Ciampa A, et al. High-performance road-vehicle optimised aerodynamic design: Application of parallel computing to car design. Future Generation Computer Systems 1999; 15: 323–332.

[11] Hucho WH, Sovran G. Aerodynamics of Road Vehicles. Annual Review of Fluid Mechanics 2003; 25: 485–537.

[12] Ozawa H, Nishikawa S, Higashida D. Development of aerodynamics for a solar race car. JSAE Review 1998; 19: 343–349.

[13] Schenkel FK. The Origins of Drag and Lift Reductions on Automobiles with Front and Rear Spoilers. SAE Technical Papers. Epub ahead of print February 1, 1977. DOI: 10.4271/770389.

[14] Ramakrishnan V, Soundararaju D, Jha P, et al. A Numerical Approach to Evaluate the Aerodynamic Performance of Vehicle Exterior Surfaces. In: SAE 2011 World Congress & Exhibition. SAE International. Epub ahead of print April 2011. DOI: https://doi.org/10.4271/2011-01-0180.

[15] Gilhaus A. The influence of cab shape on air drag of trucks. Journal of Wind Engineering and Industrial Aerodynamics 1981; 9: 77–87.

[16] Çengel YA, Cimbala JM. Fluid Mechanics: fundamentals and applications. 4th Edition. McGraw Hill, 2018.

[17] White FM. Fluid Mechanics 8e In SI Units. 8 th Edition. Mc Graw Hill, 2016.

[18] Vazirian MM, Charpentier TVJ, de Oliveira Penna M, et al. Surface inorganic scale formation in oil and gas industry: As adhesion and deposition processes. Journal of Petroleum Science and Engineering 2016; 137: 22–32.

[19] Streitberger H-Joachim, Kreis Winfried. Automotive paints and coatings. 2008; 493.

[20] Keleş U. CFD analysis of a tractor-trailer models drag coefficient under crosswind effect. Yildiz Technical University, 2015.

[21] Launder BE, Spalding DB. The numerical computation of turbulent flows. Computer Methods in Applied Mechanics and Engineering 1974; 3: 269–289.

[22] Truck, Aerodynamics B, Committee FE. Guidelines for Aerodynamic Assessment of Medium and Heavy Commercial Ground Vehicles Using Computational Fluid Dynamics. Epub ahead of print June 2021. DOI: https://doi.org/10.4271/J2966_202106.